SIMULATION ON THE THERMAL CONTRACTION COORDINATION BEHAVIOR BETWEEN ASPHALT MIXTURE OVERLAY AND GRADED GRAVEL BASE LAYER

T WAN[1], H WANG[1]*, P ZHANG[1], X YANG[1] and Y CHEN[1]

[1]School of Highway, Chang'an University, Xi'an City, Shaanxi Province, China;
*Tel: (+86)13609161519; Fax: 029 82334432; E-mail: wanghn@chd.edu.cn

ABSTRACT

The thermal contraction performance of asphaltic pavement structure is affected by the interaction between the bituminous layer and the granular layer underneath. The constraint action of the graded gravel base layer plays an important role in affecting the temperature strains in top asphalt layer. The focus of the present paper is to investigate the interactive thermal contraction mechanisms between the asphalt and granular base layers from a novel perspective. In this paper, a type of composite structure was proposed, and the dynamic and static strain acquisition system (DSSAS) was adopted to conduct the indoor thermal contraction tests. Combining the discrete properties of graded gravel materials (UAM) and the continuous characteristic of asphalt mixtures, the Finite Difference Method and Discrete Element Method (FDM-DEM) coupling models were established and calibrated. And the linear elastic and elastoplastic models of graded gravel layer were compared. Results show that the continuous-discrete coupling model has higher consistency with the laboratory test than the continuum model, and the relative error of thermal contraction coefficient is no more than 8.1%. The thermal strain-time curves of asphalt mixture and its composited specimens exhibit a nonlinear change law of first fast and then slow. And the asphalt mixture types and cooling temperature differences have little effect on the constraint action of unbound aggregate layer. The coordinated deformation between unbound aggregate base layer and asphalt mixture overlay can be realized by particle contact recombination, the inwardly extruded movement, loose on both ends and the middle compaction. Theoretical support for the research of low temperature crack resistance of graded macadam base asphalt pavement can be found in this paper.

Keywords: Road engineering, Coordinated deformation, FEM-DEM coupling, Thermal reflective cracking, Graded gravel base, Mesoscopic response.

1. INTRODUCTION

The low temperature cracking of asphalt pavement is a typical disease in the area of low temperature and large temperature difference. When the temperature of pavement structure decreases, especially when there is a large cooling range in a short time, the temperature stress is generated due to the internal temperature gradient and the asphalt surface is constrained by the base layer when it is cooled. When the rapid accumulation of temperature stress reaches a certain degree, thermal contraction cracks are generated, which are usually distributed horizontally and at equal intervals (Sun, 2013; Marasteanu et al., 2004). At present, scholars at home and abroad focus on the low temperature cracking mechanism of asphalt binder and mixture (Feng et al., 2021; Tan et al., 2017; Canestrari et al., 2015). Sun et al. (Sun, 2020) proposed that the low temperature cracking of asphalt mixture is the result of the combined action of low thermal contraction and low

temperature relaxation. However, low temperature cracking of asphalt pavement is not only a problem of the material itself, but also related to the coordinated deformation and interlayer bonding of the base layer (Sun, 2013; Dave et al., 2013; Sun et al., 2018). A thorough understanding of the coordinated deformation of the base layer is helpful to further reveal the mechanism of low temperature cracking of asphalt pavement and guide the structural design of anti-cracking asphalt pavement in areas with low temperature and large temperature difference.

The existing research on asphalt pavement cracking at low temperature considering the effect of base structure mainly focuses on the prediction model of low temperature cracking, laboratory test of low thermal contraction of composite structure and numerical theoretical calculation. Prieto-Munoz et al. (Prieto-Muñoz et al., 2013) proposed a method to calculate the structural temperature stress of asphalt pavement with graded gravel flexible base, and took the viscoelastic properties of asphalt mixture into consideration and carried out numerical calculation verification. However, the continuous linear elastic model was still adopted for graded gravel base. Sun et al. (Timm et al., 2003; Xu et al., 2014) simplified the limiting action of base layer into linear and nonlinear friction behavior, and put forward the theoretical calculation and finite element model of thermal contraction crack of asphalt surface. This method is convenient for mathematical derivation, but oversimplifies the real force of the base. In addition, Tan et al. (Xu et al., 2014) proposed a test method for low thermal contraction test of double-layer and three-layer structures to evaluate the effect of asphalt mortar interlayer on reducing the constraint and thermal contraction stress of asphalt mixture layer by limiting the strain index. Wu et al. (Sun et al., 2018; Wu, 2016) studied the constraint deformation effect of semi-rigid base by using the micrometer method through the thermal contraction test of the composite specimen of semi-rigid base and asphalt mixture layer. It is found that the constraint effect of the base layer on the surface layer is an important reason for the thermal shrinkage cracking. However, there are few experimental studies on the mechanism of structural shrinkage cracking at low temperature considering the effect of graded gravel base.

Graded macadam material is often used as the base, base and transition layer of asphalt pavement structure, which has good cracking resistance, frost resistance, drainage and diffusion stress (Ahmed et al., 2021; Cao, 2018). Due to its own granular material characteristics, it can effectively curb load-type reflection cracks and alleviate uneven deformation of subgrade (Su et al., 2017; Wang et al., 2015). As for the position of flexible pavement base or flip pavement transition layer, the mechanism of coordinated deformation in the process of low thermal contraction cracking of asphalt pavement remains to be studied (Liu). Feng et al. (Ma, 2011; Ma et al., 2015) predicted the low temperature cracking interval of asphalt pavement based on the NCHRP1-37A TC low temperature cracking model, and found that the low temperature cracking interval of graded gravel base asphalt pavement was smaller than that of asphalt stable gravel base and semi-rigid base, that is, the low temperature cracking was more serious. However, according to the one-dimension and two-dimensional temperature stress calculation theory proposed by Canestrari and Buttlar et al. (Marasteanu et al., 2004; Dave et al., 2013; Yin et al., 2005), it is found that graded gravel has advantages in the crack spacing of surface layer and can effectively reduce the crack density of pavement at low temperature. In existing studies, graded gravel layers are generally considered as continuous media materials, but the dispersion and heterogeneity of graded gravel materials are not taken into account (Chen et al., 2018; Zhang et al., 2018; Wang, 2017), which may lead to a shallow understanding of the coordinated deformation of graded gravel layers. In addition, coupling simulation of finite difference (FDM) and discrete element (DEM) has been widely applied in the field of road engineering research, with advantages of both simulation (Liu,

2020). In addition to improving the computational efficiency, the interaction law between continuous media and discrete media at mesoscale can be revealed (Jia et al., 2018; Haddad et al., 2014). Therefore, the interaction between asphalt mixture layer and graded gravel layer can be understood as the coupling effect between continuous medium and discrete medium, and the mechanism of thermal contraction coordination deformation between graded gravel and asphalt mixture can be explained from the mesoscale.

To sum up, in order to reveal the coordinated deformation behavior of low thermal contraction of composite specimens of graded gravel and asphalt mixture, two simulation model of thermal contraction test were constructed and compared in this paper, and parameters were calibrated. Combined with the thermal contraction test of indoor combined and asphalt mixture specimens, the thermal contraction deformation law and the simulation difference of continuum and continuous-discrete coupling model were compared and analyzed. The coordination mechanism of thermal contraction deformation between graded gravel and asphalt mixture was explored from micro response law level.

2. MATERIALS AND METHODOLOGY

2.1 Thermal Contraction Test

2.1.1 Composite Structure Compaction

As shown in Figure 1, indoor simulation of actual asphalt pavement paving is carried out. Three gradation types of asphalt mixture, SMA13, AC16 and AC20, were selected. Limestone was selected as the graded gravel material, and also the PC-2 slow cracking type of emulsified asphalt permeable oil. The asphalt mixture rutting plate and graded gravel mixture are formed by wheel rolling method, and the asphalt mixture rutting plate is cut into two cuboid beams with sizes of 260mm × 100mm × 50mm and 200mm × 20mm × 20mm. The latter is used for calibration (Yang et al., 2015). Then, the emulsified asphalt permeable oil was sprayed on the surface of graded gravel layer along the coincidence area (±1cm) of asphalt mixture layer and graded gravel layer in the driving direction, and the asphalt layer and graded gravel layer are bonded. The indoor composite specimen structure composed of upper layer of asphalt mixture + adhesive layer + graded gravel layer was obtained by static pressing of iron plate at room temperature at 20°C for 3 days until emulsified asphalt was demulsified.

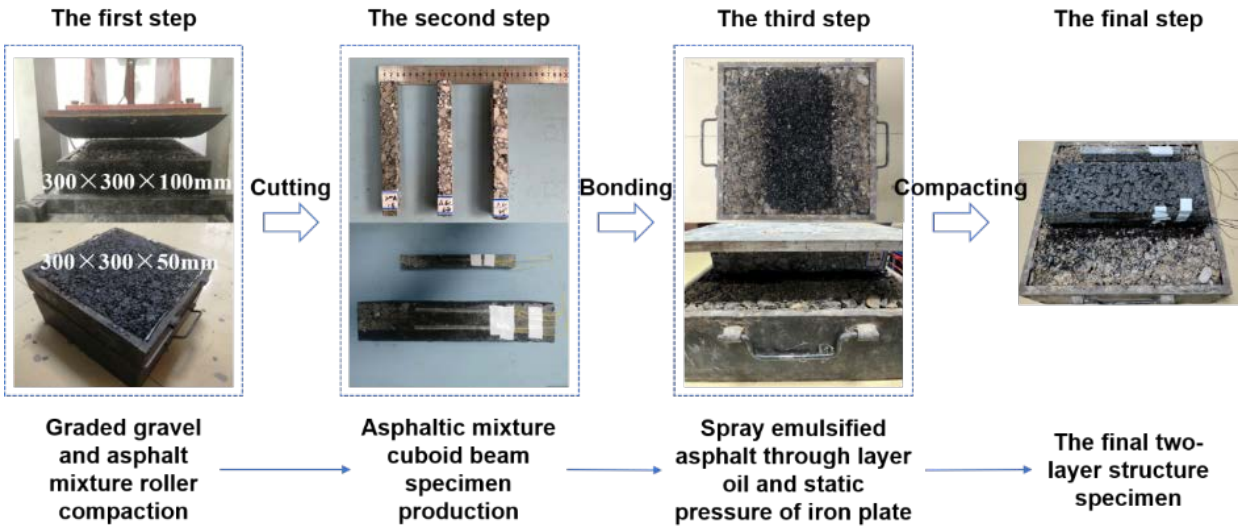

Figure 1: Molding diagram of composite structure specimen

2.1.2 Thermal Contraction Test

The DM-YB1820 dynamic and static strain acquisition system (DSSCS) was used to collect the low thermal contraction strain of composite specimens in real time. The environmental temperature control box of DTS testing machine was selected to control the cooling interval and rate. The strain gauges were BX120-80AA and 50AA. Before the test started, the strain gauge and temperature sensor were calibrated (Yang et al., 2015). The 80AA strain gauge was attached to the middle position of the side of the girder specimen at 1/5 and 3/5 height from the surface, and 50AA was attached to the middle position of the side of the trabecular specimen at 1/2 height (Sun et al., 2018), and the temperature sensor was attached to the surface of the graded gravel layer and asphalt mixture layer respectively. Spray lubricant at the bottom to ensure free shrinkage of asphalt mixture monomer specimen during the thermal contraction test, as shown in Figure 2a. The thermal contraction test of combined specimens is shown in Figure 2b.

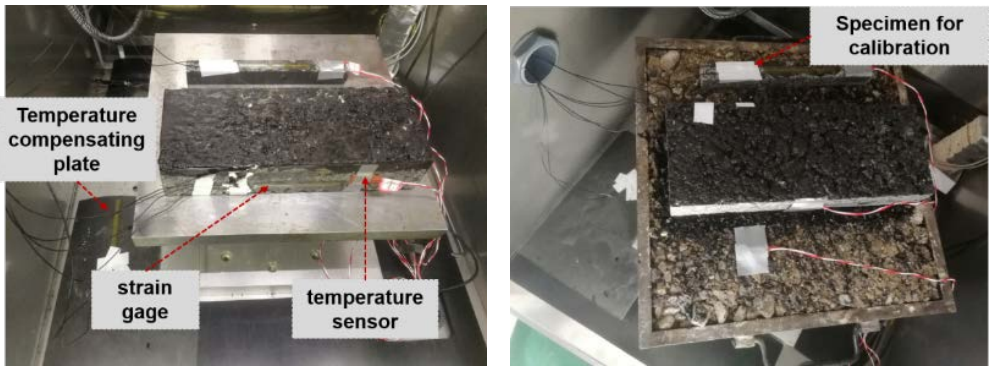

Figure 2: Thermal contraction test of (a) asphalt mixture monomer test piece and (b) composite structure specimen

The specimen was placed in an environmental chamber and kept at 10°C for 3h. The linear cooling rate is -10°C/h (Sun et al., 2018), the cooling interval is +10~-0°C, +10~-10°C and +10~-20°C, and the constant temperature is 3h when the cooling reaches the final temperature.

2.2 FEM-DEM Coupled Simulation

As shown in Figure 3, FLAC3D and PFC6.0 Suite software were used in this paper to construct a FEM-DEM coupled thermal contraction model with the same size and boundary conditions as the laboratory test. The model was composed of asphalt mixture layer, intermediate bonding layer and graded gravel layer.

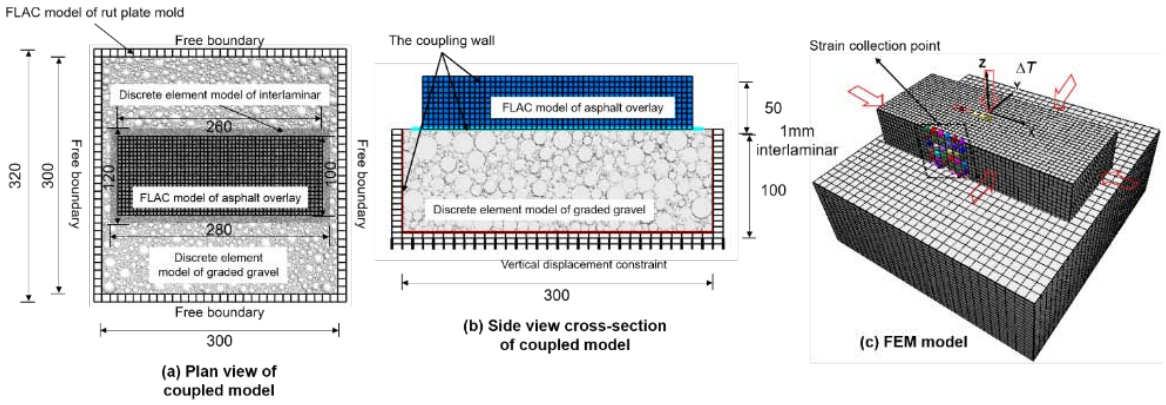

Figure 3: Schematic diagram of two simulation models (Unit: mm)

2.2.1 Asphalt Mixture Layer Model

Asphalt mixture is a viscoelastic material. When it is in a low temperature environment, its modulus is high, its relaxation ability is weak, and its mechanical response is close to linear elasticity (Sun et al., 2018; Tan et al., 2017). Therefore, linear elasticity model parameters are adopted. The elastic modulus was obtained based on the indoor static tensile test, the tensile rate was controlled to be 0.007mm/s, the tensile strain was in the range of 100με, and the modulus value at -10°C was selected as the parameter value [8]. Poisson's ratio is 0.25 in reference to the specification, and the parameters of thermal contraction test are included in Table 1 (Zhu et al., 2021; Yan et al., 2013). The mesh size is determined to be 5mmx5mmx5mm, and a total of 10400 grids are divided.

Table 1: FLAC model parameters of specimen materials

Materials	Mechanical Parameter				Thermal Contraction Paprameter	
	Elastic modulu/MPa	Possion ratio	*Friction angle c*/(°)	Cohesion φ/kPa	Conductive coefficient (W/m·K)	Heat capacity (J/ (kg·°C))
SMA13	7500	0.25	—	—	1.36	1080
AC16	8500	0.25	—	—	1.33	980
AC20	9000	0.25	—	—	1.22	900
Graded gravel	280	0.35	37.4	69.1	1.20	600

2.2.2 Graded Gravel Layer Model

2.2.2.1 Continuum Model

The linear elastic and elastoplastic models were selected for comparative analysis, and the model parameters were obtained by indoor triaxial shear test. Triaxial shear tests were carried out under confining pressures of 27.6kPa, 68.9kPa and 103.4kPa at a shear rate of 1%/min. As shown in Figure 4a, the slope of the stress-strain curve in the elastic stage is taken as the modulus value, namely the shear modulus (Li, 2015), and Poisson's ratio is 0.35 in accordance with the specification. The elastic parameters were shown in Table 1. The Mohr circle is drawn based on the Moore-Coulomb criterion, and the internal friction Angle φ and cohesion force c of graded gravel are obtained, as shown in Figure 4b. Li (Li & Hao, 2020) proposed that the graded gravel layer has a tensile strength of about 10kPa, so 10kPa tensile stress is considered in the elastic-plastic model.

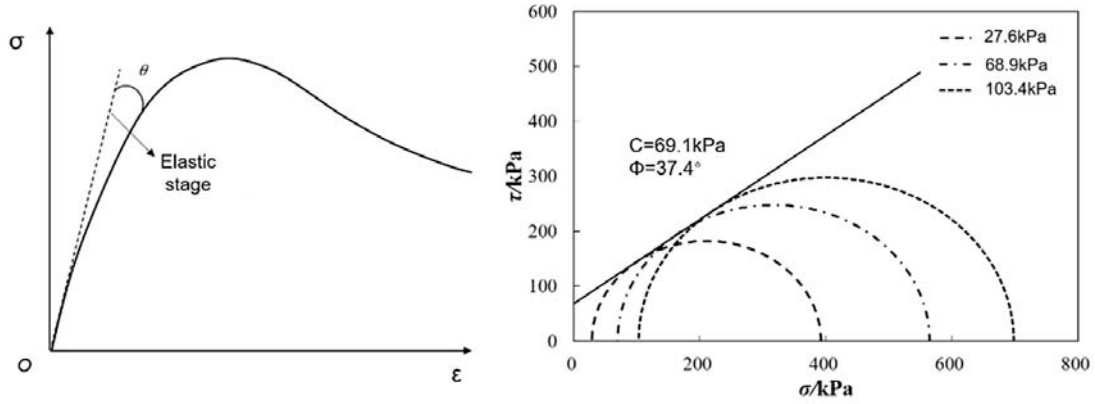

(a) (b)

Figure 4: Triaxial shear test of unbound aggregates: (a) typical stress-strain curve; (b) Mohr circle

2.2.2.2 Discrete Element Model

As shown in Figure 5, the discrete element linear contact model is used to simulate the contact between graded gravel particles and particles (Liu et al., 2013), wherein fine particles with a particle size below 1.18mm are set as particles with a particle size equal to 1.18mm, and particles with a particle size above 1.18mm are proportioned to generate the final graded gravel mixture according to the original gradation, and triaxial shear simulation is conducted. Compared with the stress-strain curve obtained by indoor triaxial shear, the mesoscopic parameters of the discrete element model of graded gravel are finally calibrated, as shown in Table 2.

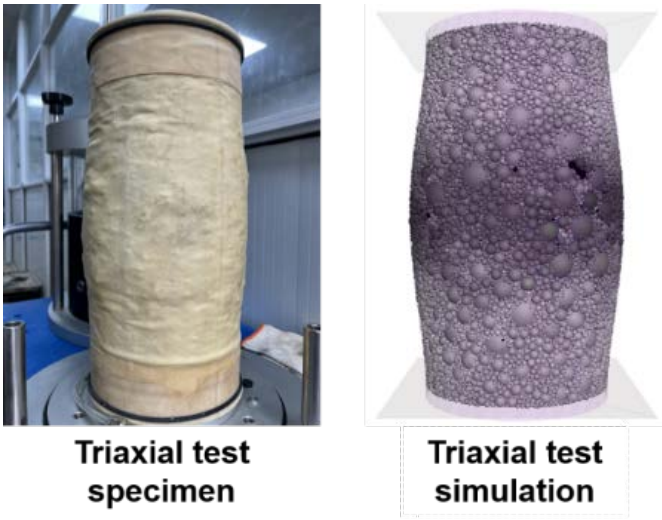

Figure 5: Triaxial shear test of unbound aggregates

2.2.3 Interlayer Bonding Model

A spherical particle with a size ranging from 0.5 to 1.0mm was generated by the "distribute" command, and a parallel bonding model was assigned between particles (Li, 2015). Parameters of the model were shown in Table 2.

Table 2: Discrete element model parameters of unbound aggregates layer and inter bonding layer

Model	Parameters	Value
Graded gravel layer	Density/(kg·m^{-3})	2600
	Damping ratio	0.7
	Porosity	0.24
Interlayer	Density /(kg·m^{-3})	2200
	Damping ratio	0.7
	Porosity	0.01
Parallel bonding	Modulus/MPa	100
	Normal bond strength/MPa	100
	Tangential bond strength/MPa	100
	Contact stiffness ratio	1.0
	Friction coefficient	0.35
Linear bonding	Modulus /MPa	450
	Contact stiffness ratio	1.4
	Friction coefficient	0.45

2.2.4 Contact Model and Boundary Condition

The vertical displacement and temperature load boundary distribution at the bottom of the composite structure model are constrained by displacement boundary, as shown in Figure 3c. Assuming that the graded gravel layer does not consider thermal contraction, only consider the shrinkage deformation of the surface layer. Temperature load is applied by assigning temperature boundary. In the FEM-DEM coupling model, linear contact model between graded gravel particles and test mode and parallel bonding contact model between graded gravel particles and bonding layer particles are given, and bonding layer particles and asphalt mixture layer are made parallel bonding contact through coupling wall.

3. RESULTS AND CONCLUSION

3.1 Thermal Contraction Behavior of Specimens

In order to compare and analyze the thermal contraction deformation behavior of different asphalt mixtures and their combination specimens. Two indicators, thermal contraction coefficient α and restraint strain coefficient *R*, were proposed and calculated using formular (1) and (2). The results were listed in Table 3.

$$a_1 = \frac{\varepsilon_t - \varepsilon_0}{t - t_0} \tag{1}$$

$$R = \frac{\alpha_1 - \alpha_2}{\alpha_1} \tag{2}$$

Where α_1 is the mean value of the thermal contraction coefficient of asphalt mixture specimen; α_2 stands for the mean value of the thermal contraction coefficient of combination specimens; ε_t is the shrinkage strain acquired in real time; ε_0 is the initial thermal shrinkage strain; t is the final temperature; t_0 is the initial temperature.

As can be seen in Table 3, the results of α and *R* of specimens were described and compared. It can be found that the larger the temperature difference is, the larger the shrinkage coefficient is and the larger the limiting strain is, but the limiting strain coefficient of the graded gravel layer increases slightly. At the same time, the limited strain coefficients of the three types of asphalt mixture specimens are basically no difference, indicating that the material parameters of asphalt mixture have little influence on the limited deformation ability of the graded gravel layer, which is an inherent attribute of the graded gravel layer. The average shrinkage coefficient of SMA13 is around 3.5×10^{-5}/°C, and the average shrinkage coefficient of AC16 and AC20 is around 2.95×10^{-5}/°C and 2.5×10^{-5}/°C, respectively, which are all within the reasonable range of 2.0×10^{-5}~5.0×10^{-5}/°C of asphalt mixture [31]. Material parameters can be provided for simulation.

Table 3: Thermal contraction behavior of asphalt mixture and its combination

Type of Specimens	Thermal Contraction Coefficient / (10^{-6}/°C)			Restraint Strain Coefficient		
	10~0°C	10~-10°C	10~-20°C	10~0°C	10~-10°C	10~-20°C
SMA13-1/5	36.2	41	42.8			
SMA13-3/5	32.3	37.8	39.5			
Mean value	**34.2**	**39.4**	**42.1**			
SMA13 combination-1/5	30.8	36.2	38.4	**0.12**	**0.12**	**0.13**
SMA13 combination -3/5	29.3	33.6	34.7			
Mean value	**30.1**	**34.9**	**36.6**			
AC16-1/5	29.3	32.8	38.7			
AC16-3/5	26.6	27.7	29.8			
Mean value	**28.0**	**30.2**	**34.3**			
AC16 combination-1/5	26.3	27.6	31.2	**0.11**	**0.12**	**0.13**
AC16 combination -3/5	23.6	25.6	28.3			
Mean value	**25.0**	**26.6**	**29.7**			
AC20-1/5	25.3	26.6	31.0			
AC20-3/5	21.1	20.9	23.6			
Mean value	**23.2**	**23.7**	**27.3**			
AC20 combination -1/5	22.3	20.3	26.4	**0.10**	**0.17**	**0.11**
AC20 combination -3/5	19.5	18.8	22.3			
Mean value	**20.9**	**19.6**	**24.2**			

3.2 Validation of the FEM-DEM Coupled Model

The thermal contraction test of the FEM-DEM coupling model was simulated and verified, and the reliability of the simulation between the Molar-Coulomb (FEM-MC) model, the FEM-Linear model and the FEM-DEM coupling model was compared and analyzed, as can be seen in Figure 6. It shows that there a relatively large difference between three models, where mainly reflected in the gragded gravel layer. For the asphalt overlay, the three models all show the tendency of inward contraction with different contraction degree. For the graded grave layer, a tendency of inward pressure exsit in DEM-FEM model, while an upward pulling trend in FEM-MC model, an inward bending tendency in FEM-linear model. As we know that basically no tensile stress is transmitted in graded gravel layer. Thus, the FEM-DEM model is more realistic.

The difference of simulation results of different grade gravel models was compared, and the relative error of thermal contraction coefficient was calculated, as shown in Table 4. It was found that the coupling model had the highest agreement with the laboratory test, and the relative error was the smallest, with the error range from 1.2% to 8.1%. The second is the MC model. The error range is 0.5%~18%. Finally, the linear elastic model has an error range of 2.2%~23.7%. The analysis shows that the simulation results of the coupling model are more stable and have higher reliability.

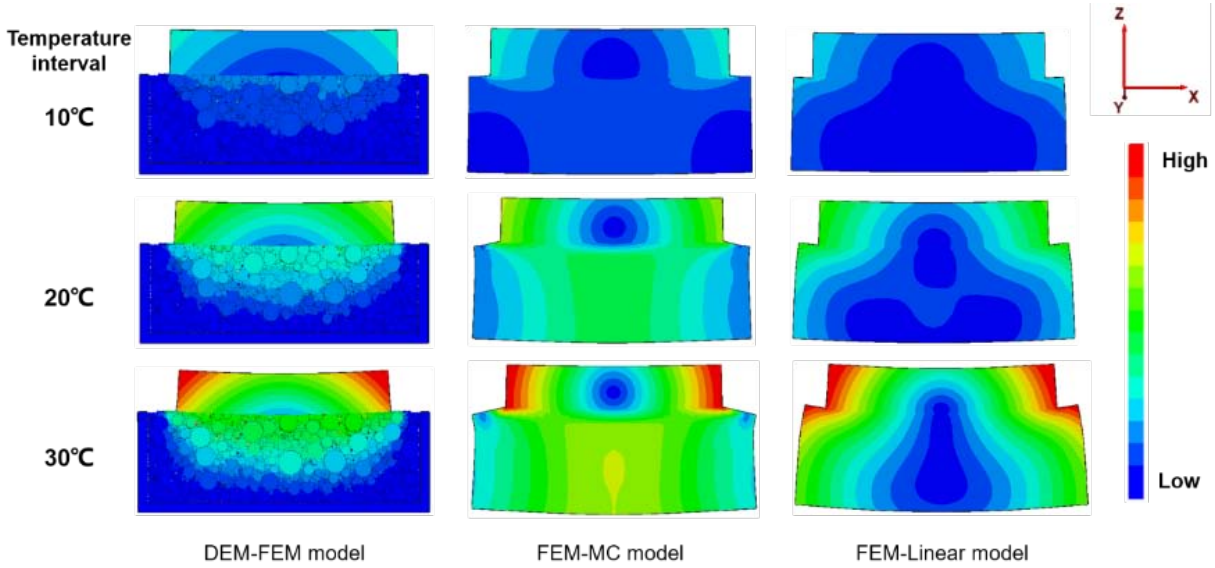

Figure 6: Thermal contraction train cloud map of three models

Table 4: Strain error of temperature shrinkage coefficient of specimens with different models

Thermal Contraction Simulation Model	Thermal Contraction Coefficient/(10^{-6}/°C)								
	SMA13			AC16			AC20		
	10°C	20°C	30°C	10°C	20°C	30°C	10°C	20°C	30°C
Indoor specimen-1/5	30.8	36.2	38.4	26.4	27.6	31.2	22.3	18.8	24.0
Indoor specimen -3/5	29.3	33.6	34.7	23.6	25.6	28.3	19.5	20.3	26.4
FEM-DEM model-1/5	32.6	37.3	37.3	26.9	29.0	30.1	21.4	20.0	25.2
FEM-DEM model -3/5	29.6	34.0	34.1	24.5	26.5	27.5	19.2	18.0	22.7
Ralative error-1/5 (%)	**-5.8**	**-3.1**	**2.7**	**-1.9**	**-4.9**	**3.7**	**3.8**	**-6.4**	**-5.1**
Ralative error -3/5 (%)	**-1.2**	**-1.2**	**1.9**	**-3.9**	**-3.5**	**2.6**	**1.5**	**6.5**	**8.1**
FEM-MC model-1/5	33.4	37.7	40.8	29.3	31.2	32.0	24.6	22.9	28.3
FEM-MC model-3/5	30.5	35.7	36.6	27.1	29.5	30.8	22.1	20.8	26.5
Ralative error -1/5 (%)	**-8.4**	**-4.1**	**-6.3**	**-11.2**	**-12.7**	**-2.5**	**-10.7**	**-21.5**	**-18.0**
Ralative error -3/5 (%)	**-4.1**	**-6.3**	**-5.4**	**-14.9**	**-15.1**	**-8.9**	**-13.4**	**-2.4**	**-0.5**
FEM-Linear model-1/5	36.3	38.9	41.5	29.8	32.1	33.3	24.9	23.3	29.3
FEM-Linear model-3/5	32.7	37.5	37.7	26.8	29.0	30.0	21.9	20.5	25.8
Ralative error -1/5 (%)	**-17.9**	**-7.5**	**-8.2**	**-13.0**	**-16.3**	**-6.8**	**-11.8**	**-23.7**	**-22.3**
Ralative error -3/5 (%)	**-11.6**	**-11.6**	**-8.5**	**-13.7**	**-13.0**	**-6.2**	**-12.3**	**-0.8**	**2.2**

3.3 Microscopic Response of Graded Gravel Layer

The movement, contact and internal structure change rules of particles inside graded gravel were visualized at mesoscale, as shown in Figure 7, and the motion displacement vector distribution of particles in graded gravel layer and bonded layer was shown in the SMA13 composite specimen model at different times. It is found that the particle displacement of graded gravel layer is mainly concentrated in the middle position, which shows the state of extrusion and bending toward the middle. The particles of the cohesive layer are drawn to the middle, which can explain the displacement and deformation of the particles of the cohesive layer in the upper section. With the passage of time, the particle movement displacement increases. The changes were obvious in the first 1h, but slight after 1h, which was consistent with the macroscopic deformation law. As shown in the marked place of the coil, in the later stage of thermal contraction deformation, particle displacement around the graded gravel layer gradually changed from a uniform distribution state at the beginning to an uneven state focusing on the left movement, indicating that the movement of particles on the left side was more obvious.

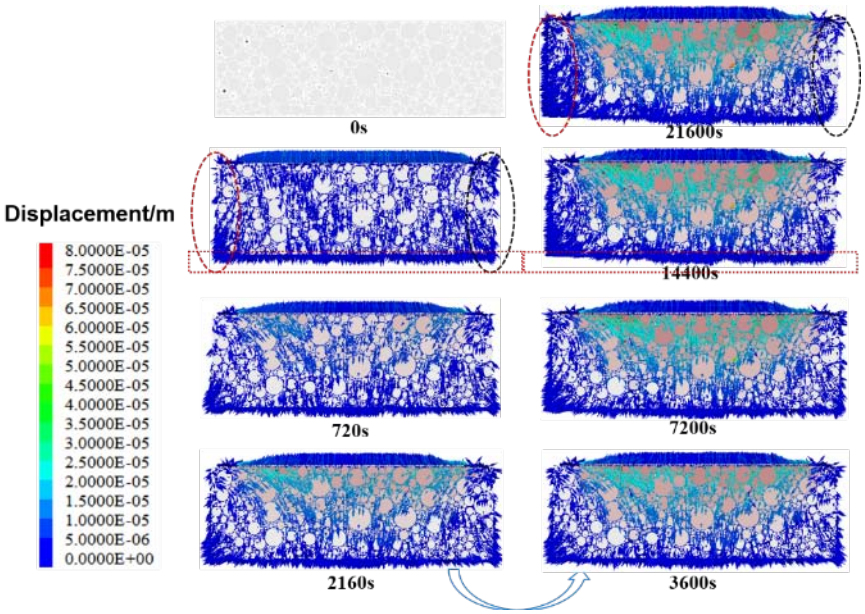

Figure 7: Schematic diagram of particle displacement vector of graded gravel layer at different time stages

4. CONCLUSIONS

In this paper, the indoor thermal contraction test of asphalt mixture and its composite specimen was designed by combining laboratory test and simulation, and the FEM-DEM coupling composite specimen model was constructed and verified. The mechanism of low thermal contraction coordination deformation of the composite structure of graded gravel and asphalt mixture is revealed from the microscale, and the main conclusions are as follows:

1) In the process of thermal contraction test, the thermal contraction strain of asphalt mixture is as follows: SMA13 > AC16 > AC20. The limited strain coefficient of the intermediate gravel layer on the asphalt mixture layer is about 0.11, which is basically not affected by the parameters of the asphalt mixture layer.

2) The thermal contraction test results of FEM-DEM coupled model are consistent with the results of laboratory test with high coincidence, and the relative error of thermal contraction coefficient is up to 8.1%. Compared with the FEM-MC and FEM-Linear continuous media models, it has the advantages of visualized particle motion and contact force chain distribution in the intermediate gravel layer of composite specimens.

3) In the early stage of coordinated deformation between the graded gravel layer and the asphalt mixture layer, the particles in the contact area of the two layers move inward, and the number of particles increases, which is in the compaction stage. The loose expansion of the particles occurred at the rear ends and the bottom, and the particle recombination was realized. In the stable stage of thermal contraction deformation, the particle movement recombination is completed, and the graded gravel layer basically does not limit the shrinkage deformation of asphalt mixture layer.

5. REFERENCES

Ahmed, I, Thom, N, Zaidi, SBA, Ahmed, N, Carvajal-Munoz, JS, Rahman, T & Ahmad, N. 2021. A mechanistic approach to evaluate the fatigue life of inverted pavements. *Construction and Building Materials,* 311:125288.

Canestrari, F, Stimilli, A, Bahia, HU & Virgili, A. 2015. Pseudo-variables method to calculate HMA relaxation modulus through low-temperature induced stress and strain. *Materials & Design,* 76:141-149.

Cao M. 2018. *Analysis on structural characteristics and load responses for rigid and flexible composite base asphalt pavement.* Ph.D, Southwest Jiaotong University.

Chen, J, Chu, R, Wang, H & Xie, P. 2018. Experimental measurement and microstructure-based simulation of thermal conductivity of unbound aggregates. *Construction and Building Materials,* 189:8-18.

Dave, EV, Buttlar, WG, Leon, SE, Behnia, B & Paulino, GH. 2013. IlliTC–low-temperature cracking model for asphalt pavements. *Road Materials and Pavement Design,* 14:57-78.

Feng, D, Cui, S, Yi, Y & Wang, D. 2021. Low temperature performance evaluation indexes of asphalt binder based on EBBR test. *Journal of Traffic and Transportation Engineering,* 21(5):94-103.

Haddad, H, Guessasma, M & Fortin, J. 2014. Heat transfer by conduction using DEM–FEM coupling method. *Computational Materials Science,* 81:339-347.

Jia, M, Yang, Y, Liu, B & Wu, S. 2018. PFC/FLAC coupled simulation of dynamic compaction in granular soils. *Granular Matter,* 20:1-15.

Li, G. 2015. *Research on the bonding behavior between graded crushed stone and asphalt layer and the impact of road performance.* Chongqing Jiaotong University.

Li, S. & Hao, P. 2020. Stress dependent and redistribution behaviour of unbound granular material. *International Journal of Pavement Engineering,* 21:347-356.

Liu, Y, You, Z, Li, L & Wang, W. 2013. Review on advances in modeling and simulation of stone-based paving materials. *Construction and Building Materials,* 43:408-417.

Liu, Y, Zhao, M, Wu, C, Wu, H, Gong, F, Su, P & Hu, C. 2020. Coupled discrete-continuous simulation and analysis of dynamic interactions between hammer and pavement. *China Journal Highway and Transportation,* 33(206):150-162.

Liu, Z. 2017. *Research on Post-evaluation of Expressway Asphalt Pavement Technology in Hebei Province*. Hebei Transportation Planning and Design Institute.

Ma, H. 2011. *The verification and improvement on asphalt pavement low temperature cracking perdiction model of AASHTO.* Master, Harbin Institute of Technology.

Ma, H, Wang, D, Zhou, C & Feng, D. 2015. Calibration on MEPDG low temperature cracking model and recommendation on asphalt pavement structures in seasonal frozen region of China. *Advances in Materials Science and Engineering,* 2015.

Marasteanu, MO, Li, X, Clyne, TR, Voller, V, Timm, DH & Newcomb, D. 2004. Low temperature cracking of asphalt concrete pavement.

Prieto-Muñoz, PA, Yin, HM & Buttlar, WG. 2013. Two-dimensional stress analysis of low-temperature cracking in asphalt overlay/substrate systems. *Journal of Materials in Civil Engineering,* 25:1228-1238.

Su, N, Xiao, F, Wang, J & Amirkhanian, S. 2017. Characterizations of base and subbase layers for Mechanistic-Empirical Pavement Design. *Construction and Building Materials,* 152:731-745.

Sun, H. 2013. Mechanical analysis of asphalt pavement low temperature cracking. Ph.D, Chang'an University.

Sun, Z. 2020. *The thermal cracking mechanism of asphalt mixtures based on the contraction-relaxation competition.* Ph.D, Harbin Institute of Technology.

Sun, Z, Xu, Y, Tan, Y, Zhang, L, Xu, H & Meng, A. 2018. Investigation of sand mixture interlayer reducing the thermal constraint strain in asphalt concrete overlay. *Construction and Building Materials,* 171:357-366.

Tan, Y, Sun, Z, Gong, X, Xu, H, Zhang, L & Bi, Y. 2017. Design parameter of low-temperature performance for asphalt mixtures in cold regions. *Construction and Building Materials,* 155:1179-1187.

Timm, D, Guzina, BB & Voller, VR. 2003. Prediction of thermal crack spacing. *International Journal of Solids and Structures,* 40:125-142.

Wang, H. 2017. *Research on dynamic triaxial numerical simulation of graded broken stones based on three - dimensional discrete element method.* Chang'an University.

Wang, H, Zhang, R, Zhou, J, Liu, Y & You, Z. 2015. Numerical simulation of deformation mechanism of geocell reinforced gravel base course. *Journal of Central South University, (Science and Technology),* 46:4640-4646.

Wu, Q. 2016. *Research on asphalt pavement structure combination in order to control transverse cracking rate.* Harbin Institute of Technology.

Xu, Y, Shan, L & Sun, Z. 2014. Effect of a sand mix interlayer on thermal cracking in overlays. *Journal of Materials in Civil Engineering,* 26:04014049.

Yan, X, Li, X, Sun, Y & Xu, D. 2013. Heat conduction epertiment of asphalt mixture based on fourier's heat conduction law. *Journal of Traffic and Transportation Engineering,* 000:1-6.

Yang, G, Wang, X & Zhang, C. 2015. A method for measuring temperature shrinkage characteristics of asphalt mixture based on real-time temperature-strain acquisition. *Journal of China and Foreign Highway,* 035:259-262.

Yin, H, Buttlar, W & Paulino, G. A two-dimensional elastic model of pavements with thermal failure discontinuities. Proc., 3rd MIT Conf. Comput. Fluid Solid Mech, 2005. 539-542.

Zhang, Y, Gu, F, Luo, X, Birgisson, B & Lytton, RL. 2018. Modeling stress-dependent anisotropic elastoplastic unbound granular base in flexible pavements. *Transportation Research Record,* 2672:46-56.

Zhu, H, Lei, L, Fan, S & Chen, R. 2021. Review of research on influence factors of asphalt pavement thermal Stress. *Science Technology and Engineering,* 21:13.